DOE/OR/45505-2

Surface morphology of laser superheated Pb(111)

Z. H. Zhang, Bo Lin, X. L. Zeng, and H. E. Elsayed-Ali[1]
Department of Electrical and Computer Engineering
Old Dominion University
Norfolk, VA 23529

The step density on the vicinal Pb(111) surface after laser superheating and melting is investigated using reflection high-energy electron diffraction. The (00) beam profiles parallel and perpendicular to the incident beam are analyzed. For laser heating with ~ 100 ps laser pulses, surface superheating does not significantly change the density of the steps and step edge roughness. A sudden increase in the average terrace width is observed after laser surface melting. The average terrace width and the string length at the step edge become as large as those at room temperature. The average terrace width at 573 K changes from 38±15 to 64±19 Å after laser surface melting, while the average string length at the step edge changes from 50±12 to 250±38 Å.

PACS: 68.35.Rh, 68.35.Bs, 61.14.Hg, 42.62.Hk

---

[1]Corresponding author, Fax: (757) 683-3220, e-mail: elsayed-ali@ece.odu.edu

DISCLAIMER

DISCLAIMER

For many years, it has been believed that melting is initiated at the surface and that, like crystallization, it occurs by nucleation and growth of defects. The primary factor governing surface melting is the interfacial free-energy difference between the ordered solid surface and the surface wetted by its melt [1],

$$\Delta\gamma = \gamma_{sv} - \gamma_{sl} - \gamma_{lv}$$

where γ_{sv}, γ_{sl}, γ_{lv} are the solid-vapor, solid-liquid, and liquid-vapor interfacial free energies, respectively. For $\Delta\gamma > 0$, the free energy of the surface is reduced by the formation of a thin disordered layer when the temperature is below the melting point, T_m, and surface premelting occurs. Supercooling of the melt is a well-demonstrated phenomenon attributed to a nucleation barrier to solidification that is a result of the increase in free energy due to the formation of a solid-liquid interface. Superheating of solids, however, is rarely observed due to the presence of a thin disordered surface layer formed below T_m, which provides a nucleation site for melting. The general trend is that close-packed surfaces do not premelt while open surfaces disorder below T_m. While the top atomic layer of Pb(110) disorders at a temperature as low as 150 K below T_m, Pb(111) remains ordered up to T_m [2,3]. This was confirmed by medium-energy ion scattering experiments on Pb(111), and its vicinal surfaces, performed at temperatures up to T_m - 0.05 K [3]. A sudden increase in terrace width on the Pb(111) surface was observed above 580 K [4].

Superheating of Pb{111} bounded microcrystallites by a few degrees above T_m was previously observed [5]. More recently, superheating of Pb(111) and Bi(0001), and some superheating of Pb(100) by ~ 180 ps laser pulses was observed in time-resolved reflection high-energy electron diffraction (RHEED) experiments [6-8]. During and following pulsed laser irradiation, the surface superheats up to ~ 120 K and ~ 90 K above the bulk melting point of Pb and Bi, respectively. In contrast, the open Pb(110) surface premelts for similar laser heating conditions [9]. For the Pb(100) surface, evidence of residual order above T_m was also observed [7].

Using molecular dynamics (MD) simulations, the surface melting behaviors of several fcc metals were modeled [10,11]. Tolla et. al. modeled the melting of Al(111) using the glue potential, which is expected to be an accurate treatment for noble metals.

Superheating by 149±18 K was observed even for very long MD runs extending up to 2 ns [10]. This model showed good agreement with the experimentally observed superheating of Pb(111) [6]. Häkkinen and Landman used the many-body embedded atom potential to simulate pulsed laser heating of Cu(110) and Cu(111) [11]. The reason why they chose Cu rather than Pb, as in the experiments of Herman and Elsayed-Ali [6], was the availability of accurate parameters for the embedded atom potential in the case of Cu. In their model, superheating of Cu(111) by 40 K above T_m was observed, while Cu(110) melted. An interesting observation was that even a highly damaged Cu(111) surface, with as much as 10% preexisting vacancies, could also be superheated. This is surprising, since melting nucleates at defects, a highly defective surface is not expected to superheat. However, the MD simulations showed that this large concentration of vacancies and adatoms anneal through a non-diffusional, cooperative mechanism in which the adatoms settle in the top layer, while the cooperative surface atom movement results in the filling of vacancies. The surface became atomically flat. Thus, superheating was shown to repair the surface [11]. This surface annealing mechanism was attributed to the high vibrational amplitudes which atoms are forced into by the ultrafast superheating pulse.

We have investigated surface step density after laser superheating of Pb(111) using RHEED. We used similar experimental conditions as those previously used in time-resolved RHEED experiments on superheating of Pb(111) [6]. The present experiments were initiated in order to investigate the proposed surface annealing by superheating [11]. By carefully analyzing the RHEED intensity profile, the average surface step terrace size can be obtained [12,13]. Pb(111) maintained at 573 K, T_m = 600.7 K, was heated by a pulsed laser with a pulse width of ~ 100 ps measured at full-width at half maximum (FWHM). After laser superheating, we find that the average terrace width and the average string length at the step-edge increase and become as large as those at room temperature. The terrace width is defined as the distance of a flat surface area between an up and a down pair of steps. The string length is the length of a straight line of atoms at a step edge, bounded by an up and down atomic steps at the edge. A sudden increase in terrace width is achieved when the laser fluence is high enough to cause surface melting after superheating.

An ultrahigh vacuum chamber equipped with RHEED and Auger systems was used. The residual gas pressure in the chamber was less than 7×10^{-11} Torr. The electron beam energy used for RHEED was 9 keV. A single-pass cylindrical-mirror electron energy analyzer for Auger was used to check for surface impurity. A 6.4 mm diameter, 2 mm thick Pb(111) single-crystal with 99.999% purity was used. The sample surface was chemically polished and was sputtered clean at 520 K using an argon ion beam with 1.5 - 2 keV energy. After sputtering and annealing the sample at 500 K for more than 10 hours, the Auger spectrum did not show any detectable impurity and we obtained a sharp 1×1 RHEED pattern of the Pb(111) surface. The temperature was measured by two thermocouples clipped onto the crystal surface. The thermocouples were calibrated to the bulk melting temperature of Pb and the boiling point of distilled water. A temperature uncertainty of ±2 K near the Pb melting point and ±1 K near the boiling point of water is estimated. Temperature stability within ±0.1 K was attained using a temperature controller.

The RHEED patterns were acquired using a charge-coupled two-dimensional array detector interfaced to a personal computer. A Nd:YAG (yttrium aluminum garnet) laser operating at a wavelength $\lambda = 1.06$ μm and a pulse width of ~ 100 ps with 50 Hz repetition rate was used to heat the sample. The temperature rise of the Pb(111) surface due to laser pulse irradiation was calculated from a one-dimensional heat diffusion model [14]. For 1 mJ laser pulse energy, the corresponding fluence on the surface is $(9.0\pm1.6)\times10^{6}$ W/cm^2. The error bar in the fluence is mainly due to the estimated spacial non-uniformity in the heating laser, which was measured to be 18% over an area equivalent to the surface area of the Pb(111) crystal. This measurement was accomplished by scanning the laser beam by a ~ 100 μm pinhole and, therefore, does not account for microscopic non-uniformity that can occur in the laser spacial profile. The laser pulse energy was varied from 2.9 to 14.4 mJ, causing a calculated peak ΔT of 45±10 K for the 2.9 mJ pulse energy.

Figure 1(a) is a RHEED pattern taken of the clean Pb(111)-1×1 surface obtained at room temperature with an electron energy of 9 keV incident along the [110] direction of the Pb crystal. The angle of incidence of the electron beam was ~ 4.1°, corresponding to the out-of-phase condition, in which the (00) beam profile is sensitive to surface steps or islands. S_x and S_y are the components of the momentum transfer parallel and perpendicular to the electron beam, respectively. Fig.1(b) is a three-dimensional RHEED intensity profile of the (00) beam in which a splitting producing two peaks along the [110] direction of the Pb crystal is observed. This indicates that surface steps are vicinal and perpendicular to the [110] direction, as schematically shown in Fig. 1(c) [13,15].The measured spacing between the two split peaks along the [110] direction is 0.246±0.07$Å^{-1}$. Taking into account the instrumental response of 0.172 $Å^{-1}$, the vicinal terrace width of the studied Pb(111) surface obtained at room temperature is 85±25 Å. The instrumental response is obtained from the full width at half maximum (FWHM) of the (00) beam at the in-phase condition [16-18]. In addition, the intensity profile perpendicular to the [110] direction was analyzed. This gives information on kinks and meanders at the step-edge. Meanders refer to a turning or winding of the step at its edge, increasing the step edge roughness. Fitting the intensity profile of the (00) beam to a Lorentzian function, a FWHM of 0.142±0.02 $Å^{-1}$ was obtained. Thus, the measured average string length at the vicinal step-edge obtained at room temperature is 220±33 Å. An instrumental response of 0.114 $Å^{-1}$ is used for the direction perpendicular to the electron beam. When the surface temperature is increased, the splitting in the peak becomes broad, indicating that the terrace width is decreased. Upon heating the surface above 543 K, the splitting in the peak disappeared and the peak profile became a Lorentzian. This is due to either an increased randomness in terrace width or meandering at step edges, in particular, near the bulk melting point [13]. At 573 K, the measured average terrace width and average string length decrease to 42±17 Å and 70±21 Å, respectively. Above 573 K, the measured average terrace width and string length continue to decrease up to 590 K. This measurement indicates that the vicinal Pb(111) surface undergoes a roughening transition at step edges due to the thermally generated meandering at step edges causing the observed changes in the average terrace width and string length and the disappearance of the splitting peak.

We next describe the change in surface step density of Pb(111) after laser superheating. The sample was first heated from 323 K to 573 K on a hot stage. RHEED patterns were acquired at different temperatures. The surface was then treated with 1000 laser pulses. This number of laser pulses was used to establish equilibrium conditions for surface roughness for a particular laser fluence as will be discussed later. A RHEED pattern was acquired after laser treatment. The sample was then cooled back to 323 K. The measurements were repeated for different laser pulse energies. RHEED profile analysis showed that the average terrace width changed after laser heating. Upon cooling back to 323 K followed by heating to 573 K, the average terrace width became nearly the same as that prior to laser treatment. This temperature recycling after laser irradiation allowed us to bring back the surface to nearly the same surface roughness conditions prior to each laser treatment. The substrate is heated from 323 K to 573 in about 10 minutes and is cooled to 323 K in approximately 45 minutes. Figure 2(a) shows one-dimensional RHEED intensity profiles of the (00) beam parallel to the [110] direction of the Pb crystal at the out-of-phase condition before and after laser heating with a laser pulse energy of ~ 14.4 mJ and a total of 1000 laser pulses. These profiles were taken at 573 K with the electron beam incident along the [110] direction. After laser heating, the peak intensity becomes larger and the FWHM of the profile becomes narrower. This indicates that the average terrace width of the steps increases. At this temperature, the profile does not show splitting, due to meandering at the step edges. RHEED profiles of the (00) beam taken perpendicular to the [110] direction of the Pb crystal, Fig. 2(b), show similar trends to those parallel to the [110] direction. This indicates that the average string length at the step edge is increased after laser heating.

The FWHM of the (00) beam intensity profiles parallel and perpendicular to the [110] direction of the Pb crystal was measured before and after laser heating. The sample was maintained at 573 K during these measurements. The average surface terrace width and the average string length at the step edge is obtained after accounting for the instrumental response. A total of 1000 laser pulses were used for each irradiation condition and laser heating was performed while the sample was kept at 573 K using a heating stage. Figure 3(a) shows that the average terrace width after laser heating does not change significantly below a laser fluence of $(9.7\pm1.7)\times10^7$ W/cm^2 corresponding to a ~ 10.8 mJ pulse energy. Above that laser fluence, the average terrace width increases from nearly 38 Å to 64 Å, becoming about the same as that at room temperature. The average terrace width was measured before each laser heating and is shown in Fig. 3(b). After laser heating at each fluence, the sample was cooled to 323 K, then thermally heated again to 573 K. The measurements reported in Fig. 3(b) are obtained prior to surface heating with the laser energy indicated. As shown in Fig. 3(b), this cooling of the sample followed by heating to 573 K results in a terrace width of ~ 40 Å. The terrace width increases after laser heating with an energy above ~ 10.8 mJ. Figure 4(a) shows the measured average string length after laser heating, which is an average of all lines of atoms at the step edge, as schematically shown in the insert. Below a laser energy of ~ 10.8 mJ, the average string length is not affected by laser heating. Above that energy, the average string length changes from ~ 50 Å to ~ 250 Å. Figure 4(b) shows that the average string length before laser heating is 70 to 100 Å. Comparing Fig. 4(a) with Fig. 4(b), a noticeable increase in the average string length is shown after heating with a laser energy above ~ 10.8 mJ. At 573 K and after laser heating, we did not observe the splitting peak as seen at room temperature, which means that the surface terrace width remains random or that the surface undergoes faceting, as discussed later, even though meandering at step edges is decreased as shown in Fig. 4(a).

Based on kinematic diffraction, we conclude that these FWHM changes in the RHEED profiles are completely due to changes in step density and step-edge roughness, not vacancies [15,19]. From these RHEED profiles, we obtain the changes in the average terrace width and string length. Without taking into account the instrumental broadening, the RHEED intensity from a two-dimensional monatomic stepped-surface is given by: [13,15]

$$I(S) = I_0(S) + I_1(S)$$
$$= e^{-2M}\{2\theta(1-\theta)[1-\cos(S_z t)]H(S_{//}, \theta) + [1-2\theta(1-\theta)][1-\cos(S_z t)]\} \quad (1)$$

where S is the momentum transfer with components parallel and perpendicular to the surface, $S_{//}$ and S_z, and e^{-2M} is the Debye-Waller factor. θ is the surface coverage, and t is the single step height. $H(S_{//}, \theta)$ is a height correlation function. $I_0(S)$ produces a diffuse intensity in the shape of a Lorentzian function with FWHM depending on step density. For a vicinal stepped-surface, the diffuse intensity is more complicated and gives a splitting shape [15]. If the surface is two-dimensional containing only vacancies, the first term becomes [13,19]

$$I_0(S) = e^{-2M} \{2\theta(1-\theta)[1-\cos(S_z t)]\}. \quad (2)$$

An increase in vacancy density causes the background intensity to increase without broadening of the RHEED profile. For Pb(111), FWHM changes were observed and imply that the step model applies to high temperature disorder of Pb(111).

For heating with a laser energy less than 10.8 mJ, we do not observe a noticeable change in the average terrace width or string length. According to our heat diffusion model, the maximum surface temperature rise due to the ~ 10.8 mJ, 100 ps FWHM, λ = 1.06 μm laser pulse is 140±37 K above T_m. Our previous time-resolved RHEED experiments on Pb(111) showed that the maximum superheating temperature was ~ 120 K [6]. This measurement was performed with ~ 180 ps FWHM laser, and did not account for convolution effects arising from the electron pulse width being about the same width as the laser heating the surface. These convolution effects reduce the observed superheating. Considering convolution effects, the ±18% estimated nonuniformity of the laser heating, the uncertainties in the values of the different parameters in the model, in addition to the shorter laser pulse used in the present experiments, we conclude that the maximum superheating is reached for ~ 10.8 mJ laser energy. At higher energies, the surface melts. Thus, superheating of the Pb(111) surface without subsequent melting does not lead to a noticeable annealing of surface steps. For laser pulse energies sufficient to cause melting after superheating, a sudden increase in the average terrace width and the average string length is observed.

The results presented in Figs. 2-4 were all obtained for surface treatment with 1000 laser pulses. Surface roughness was strongly dependent on the number of laser pulses the surface was exposed to for a particular laser fluence. Figure 5 shows the changes in the average terrace width and string length with the number of laser pulses used for a laser energy of ~ 11.7 mJ, which is above the threshold for surface melting. The changes in both the average terrace width and the average string length reach equilibrium after surface exposure to ~ 500 laser pulses. After ~ 2000 laser pulses, the average terrace width and string length decrease, indicating that surface damage starts to occur. This could be due to microscopic hot spots in the laser heating pulse causing accumulated laser damage to the surface. For a laser fluence below that required for melting, surface roughness is not affected by the laser pulses. For surface heating with a single laser pulse, we did not observe any change in the average terrace width and string length for laser energies up to ~ 14.4 mJ.

In the MD simulations of superheating of Cu(111) by Häkkinen and Landman [11], a vacancy annealing mechanism, repairing the surface through superheating, was proposed based on a non-diffusional cooperative movement of surface atoms. In this mechanism, high density of vacancy clusters are annealed by the action of adlayer islands which embed locally into the topmost layer. This mechanism is thought to be a result of the increased surface atomic vibrational amplitude by superheating. For Pb(111), our results show that superheating, by itself, does not anneal surface steps. When the threshold for superheating is exceeded and surface melting occurs, a significant reduction in step density and average string length on these steps is observed after a number of laser pulses. Pinxteren et. al. observed that for Pb(111), surface-melting-induced faceting occurs at high temperature [3]. If the surface is misoriented with respect to the (111) orientation, the surface decomposes at high temperature into dry and melted facets with a variety of orientations. In our experiment, the fact that the split in the (00) RHEED peak profile was not observed at 573 K after laser surface melting, even though there was a large increase in the average step width and string length, could be explained by facet formation. Faceting of the vicinal Pb(111) was reported in the MD simulation of Bilalbegović et. al. [20]. At room temperature, the vicinal surface of Pb(111) is a monatomic stepped surface. At T = 0.97 T_m, ~ 583 K, the vicinal surface of Pb(111) shows the occurrence of a facet with a flat, crystalline (111) surface, and a tilted, melted surface. The facet with 5 monatomic step height and a variety of orientations, between 18° and 27° away from the (111) orientation, produces a large step terrace. The broadening terrace width is approximately 1.67 times the terrace width of a monatomic step at room temperature. The equilibration time for the formation of a facet is about 1 ns. The temperature for surface-melting induced faceting in our experiments should be higher than that estimated in the MD simulation, 583 K, since we did not observe a sudden increase in the terrace width up to 590 K [21]. For a laser fluence above the surface melting threshold, facet formation can occur after surface melting. With each laser shot of ~ 100 ps measured at FWHM, the surface is heated above the melting threshold for ~ 150 ps, in which the mobility of surface atoms is much higher than that for the solid [22]. During that time, the facets can easily grow. After each laser pulse, defaceting is slow because the sample is maintained at 573 K, close to a temperature at which the facets form [3,20]. The subsequent laser pulse makes the facets grow even further. After ~ 400 laser pulses with an energy of ~ 11.7 mJ the facet size reaches an equilibrium, as shown in Fig. 5. The equilibrium terrace width after 400 pulses becomes ~ 80 Å, about twice the terrace width prior to laser melting, which is consistent with the factor of 1.67 obtained from the MD simulation [22].The change in the terrace width is ~ 40 Å, therefore, the growth rate of a terrace is ~ 0.1 Å per pulse. For 1 laser pulse, the change in the terrace width, 0.1 Å, is too small to observe. By cooling the sample to room temperature and then heating it up to 573 K, the terrace width became about the same as that prior to laser treatment. This is because at low temperature, the facet is not stable and defaceting occurs faster than that at 573 K. For a laser fluence sufficient to cause surface superheating but below the threshold for surface melting, the mobility of surface atoms remains small, consistent with that for a solid surface. Therefore, the terrace width does not change and the surface is not annealed.

In conclusion, for Pb(111) heated with ~ 100 ps laser pulses, superheating does not significantly change the average step width or the step edge roughness. A sudden increase in terrace width is achieved only when the laser fluence is high enough to cause surface melting after superheating. The average terrace width and the average string length at the step edge become as large as those at room temperature. The average terrace width at 573 K changes from 38±15 to 64±19 Å after laser heating, while the average string length at the step edge changes from 50±12 to 250±38 Å.

References and notes

1. D. P. Woodruff, The Solid-Liquid Interface (Cambridge University press, London, 1973).

2. J. W. M. Frenken, and J. F. van der Veen, Phys. Rev. Lett. **54**, 134 (1985); J. W. M. Frenken, P. M. J. Maree and J. F. van der Veen, Phys. Rev. B. **34**, 7506 (1986).

3. B. Pluis, A. W. Denier van der Gon, J. W. M. Frenken, and J. F. Van der Veen, Phys. Rev. Lett. **59**, 2678 (1987); B. Pluis, T. N. Taylor, D. Frenkel, and J. F. Van der Veen, Phys. Rev. B. **40**, 1353 (1989); H. M. Van Pinxteren and J. W. M. Frenken, Europhys. Lett. **21**, 43 (1993); H. M. Van Pinxteren, B. Pluis, and J. W. M. Frenken, Phys. Rev. B. **49**, 13798 (1994).

4. H. N. Yang, T. M. Lu, and G. C. Wang, Phys. Rev. Lett. **62**, 2148 (1989).

5. J. J. Métois and C. Heyraud, Ultramicroscopy **31**, 73 (1989); J. Phys. (Paris) **50**, 3175 (1989).

6. J. W. Herman and H. E. Elsayed-Ali, Phys. Rev. Lett. **69**, 1228 (1992); Phys. Rev. B **49**, 4886 (1994); Science News, 164, September, 1992.

7. J. W. Herman, H. E. Elsayed-Ali, and E. A. Murphy, Phys. Rev. Lett., **71**, 400 (1993).

8. E. A. Murphy, H. E. Elsayed-Ali, and J. W. Herman, Phys. Rev. B. **48**, 4921 (1993).

9. J. W. Herman and H. E. Elsayed-Ali, Phys. Rev. Lett. **68**, 2952 (1992).

10. F. D. Di Tolla, F. Ercolessi and E. Tosatti, Phys. Rev. Lett. **74**, 3201 (1995).

11. H. Häkkinen and Uzi Landman, Phys. Rev. Lett. **71**, 1023 (1993); Science News, 135, August, 1993.

12. S. Ino, Japan J. Appl. Phys. **16**, 891 (1977).

13. M. G. Lagally, D. E. Savage, and M. C. Tringides, in: "Reflection High-Energy Electron Diffraction and Reflection Imaging of Surfaces", K. Larson and P. J. Dobson, Eds., NATO ASI Series B, Phys. **188**, Plenum, 139 (1988).

14. H. E. Elsayed-Ali and J. W. Herman, Appl. Phys. Lett. **57**, 1508 (1990).

15. C. S. Lent and P. I. Cohen, Surf. Sci. **139**, 121 (1984).

16. J. M. Van Hove and P. I. Cohen, J. Vac. Sci. Technol. A **1**, 609 (1983).

17. H. N. Yang, T. M. Lu, and G. C. Wang, Phys. Rev. Lett. **62**, 2148 (1989).

18. T. M. Lu and M. G. Lagally, Surf. Sci. **99**, 695 (1980).

19. J. M. Pimbley and T. M. Lu, Surf. Sci. **139**, 360 (1984).

20. G. Bilalbegović, F. Ercolessi, and E. Tosatti, Europhys. Lett., **17**, 333 (1992).

21. Yang et. al. observed a sudden increase in terrace width at 580 K in HRLEED experiments [4]. We did not observe this sudden increase even at 590 K which maybe related to the difference in the surface morphology between the crystals used. The surface step at room temperature in the experiment of Yang et. al. shows the randomness in its terrace width since no splitting peak was observed. This is in contrast to the vicinal surface observed in our case.

22. J. W. M. Frenken, J. P. Toennies, and Ch. Wöll, Phys. Rev. Lett. **60**, 1727 (1988).

Figure Captions

Fig. 1. (a) A RHEED pattern taken of the clean Pb(111)-1×1 surface at room temperature with an electron energy of 9 keV incident along the [110] direction of the Pb crystal. The angle of incidence of the electron beam is ~ 4.1°, corresponding to the out-of-phase condition. S_x and S_y are the components of the momentum transfer parallel and perpendicular to the electron beam, respectively. (b) A RHEED intensity profile of the (00) beam. The average vicinal terrace width on Pb(111) at room temperature is 85±25 Å. The average string length at the vicinal step-edge at room temperature is 240±33 Å. © A schematic illustration of vicinal steps.

Fig. 2. (a) RHEED intensity profiles of the (00) beam taken at 573 K before and after laser heating with ~ 100 ps, ~ 14.4 mJ, 1000 laser pulses. The RHEED profiles are taken parallel to the [110] direction at the out-of-phase condition. After laser heating, the profile becomes narrower with a larger peak intensity. (b) The profiles taken of the (00) beam perpendicular to the [110] direction, which show the same trend with laser heating as for (a).

Fig. 3. (a) The average terrace width remains almost unchanged for a laser fluence of $(9.7\pm1.7)\times10^7$ W/cm^2 corresponding to a ~ 10.8 mJ pulse energy. For higher energies, it increases from ~ 40 to ~ 70 Å, becoming about the same width as that at room temperature. (b) The average terrace width before laser heating is shown to be ~ 40 Å.

Fig. 4. (a) The average string length after laser heating changes from ~ 50 to ~ 250 Å, above a laser pulse energy of ~ 10.8 mJ. (b) The average string length before laser heating varies from ~ 70 to ~ 100 Å.

Fig. 5. Changes in the average terrace width and string length with number of heating laser pulses for a laser energy of ~ 11.7 mJ which causes surface melting. (a) Average terrace width. (b) Average string length.

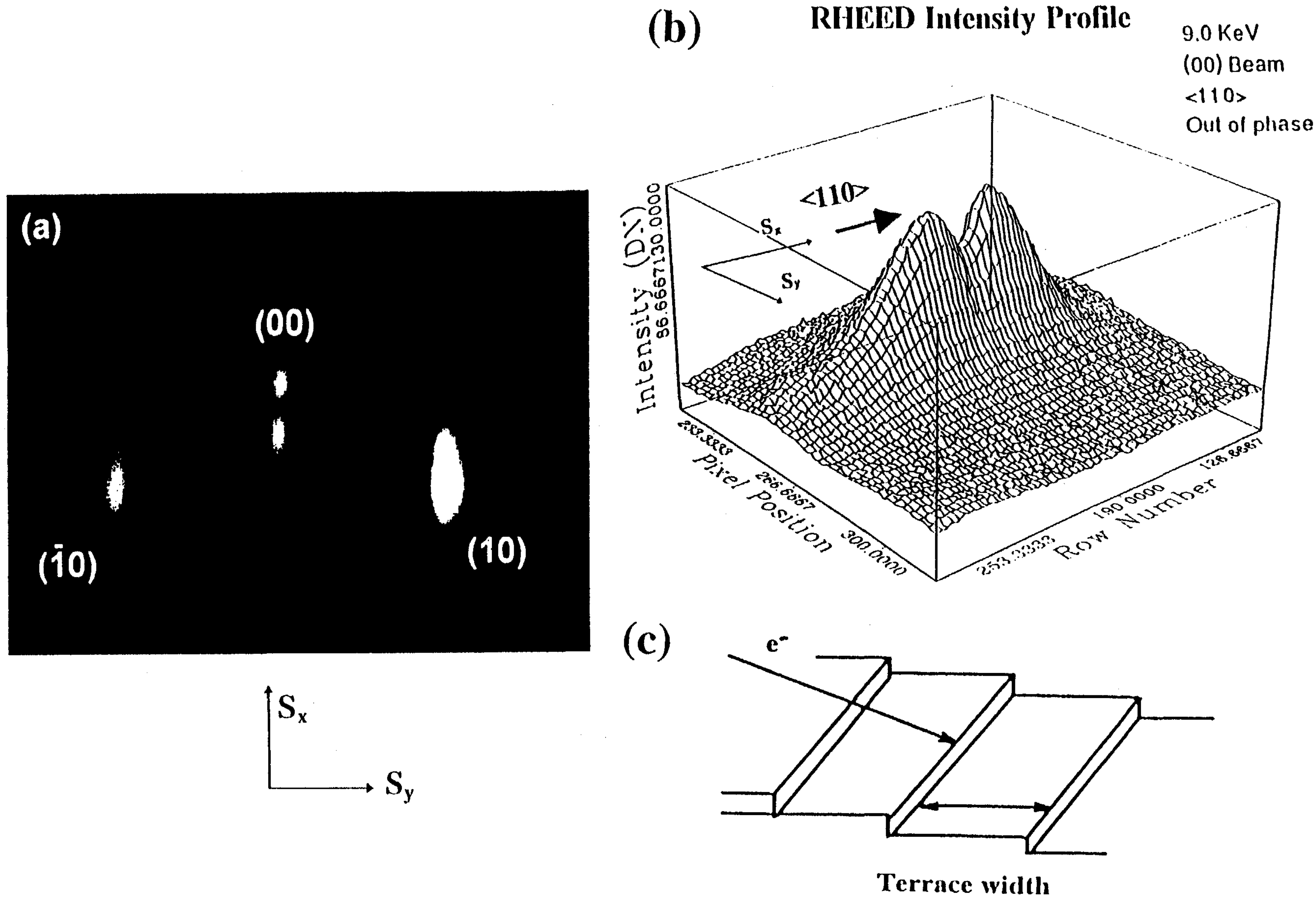

(a)
(00)
($\bar{1}$0)
(10)
S_x
S_y
(b)
RHEED Intensity Profile
9.0 KeV
(00) Beam
<110>
Out of phase
<110>
S_x
S_y
Intensity (DX)
96.6667130.0000
Pixel Position
266.6667
300.0000
Row Number
190.0000
128.8667
253.3333
(c)
e⁻
Terrace width

Fig. 1

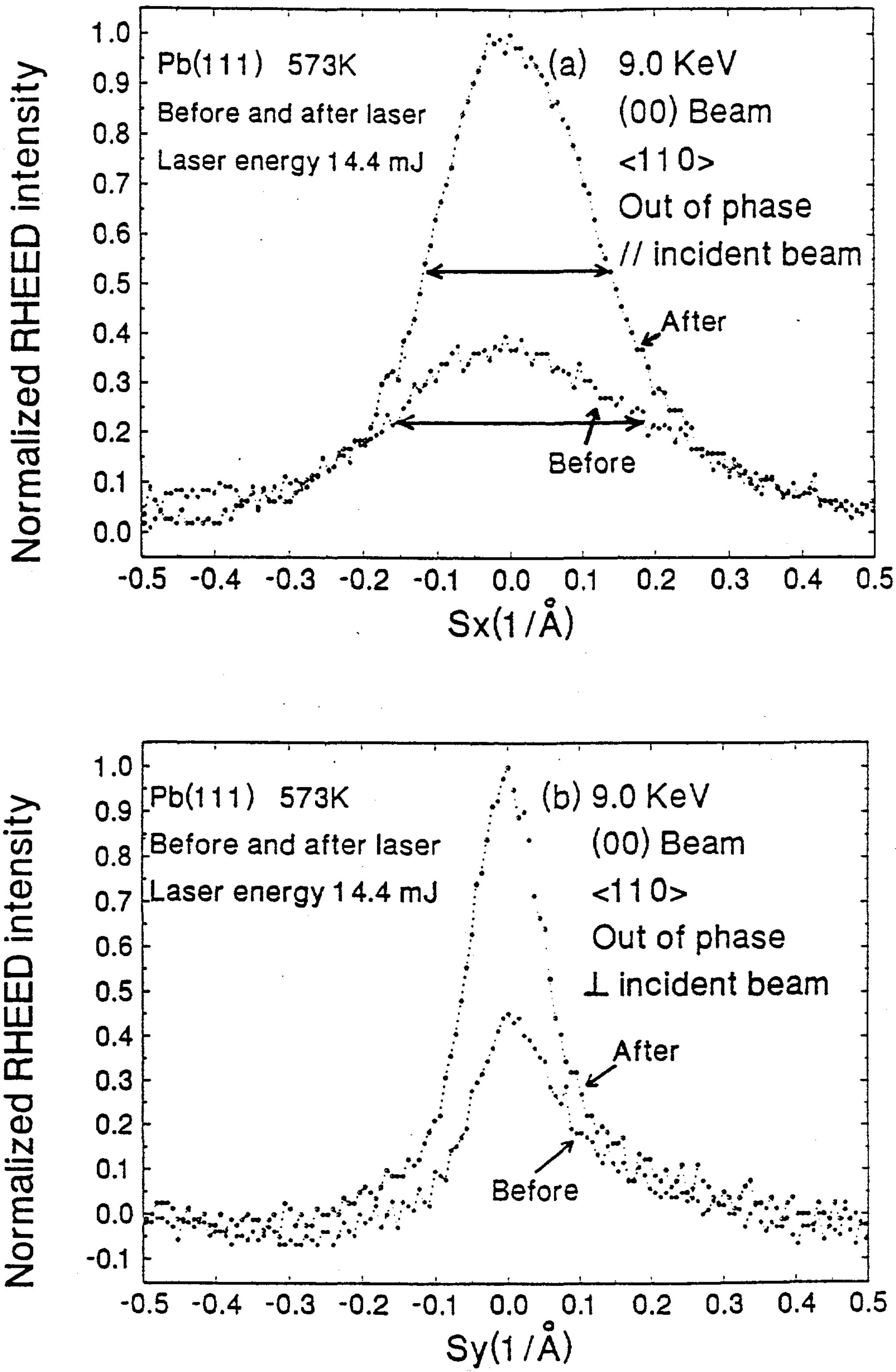
Pb(111) 573K
Before and after laser
Laser energy 14.4 mJ
(a) 9.0 KeV
(00) Beam
<110>
Out of phase
// incident beam
After
Before
Normalized RHEED intensity
Sx(1/Å)
Pb(111) 573K
Before and after laser
Laser energy 14.4 mJ
(b) 9.0 KeV
(00) Beam
<110>
Out of phase
⊥ incident beam
After
Before
Normalized RHEED intensity
Sy(1/Å)

Fig. 2

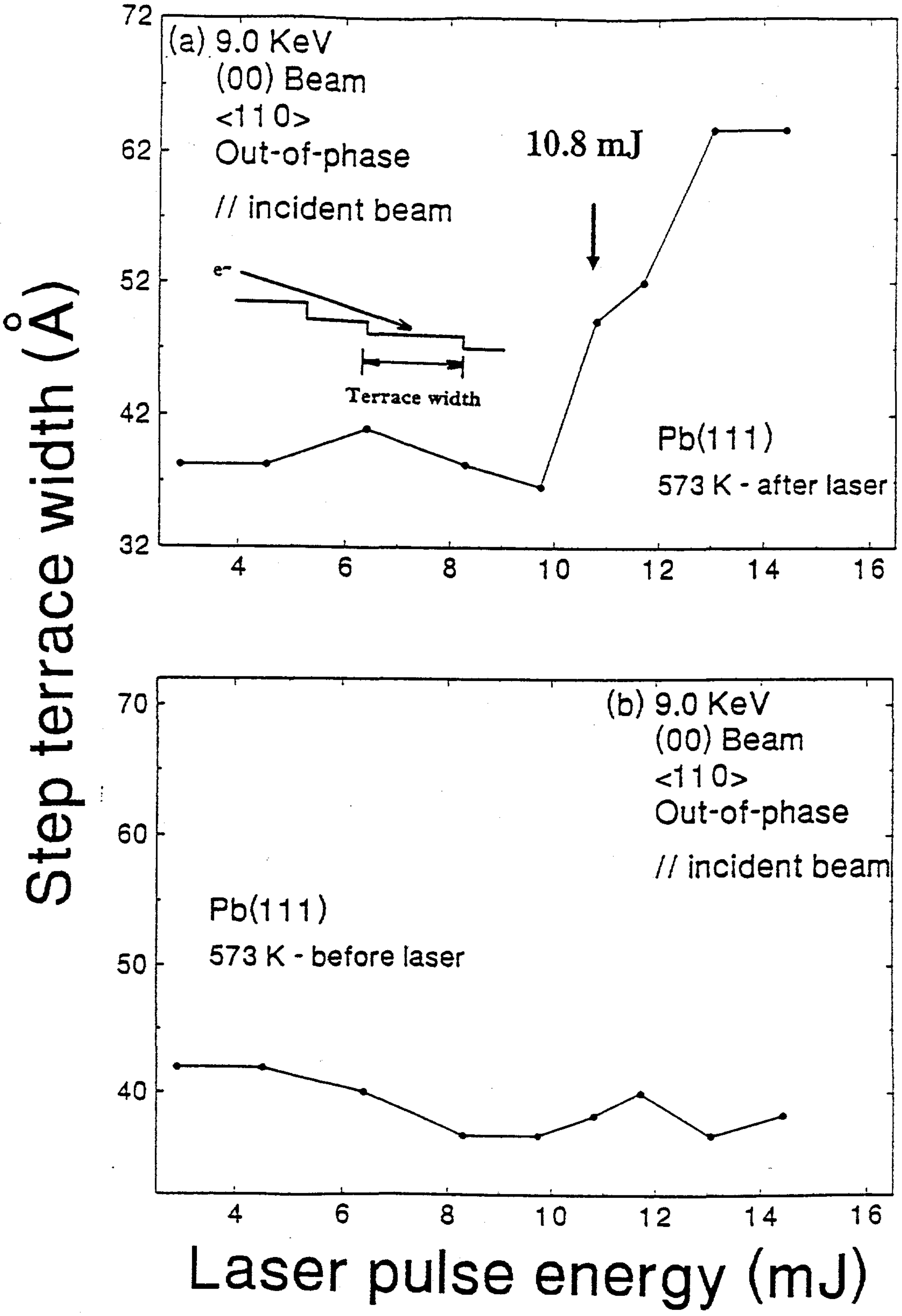
(a) 9.0 KeV
(00) Beam
<110>
Out-of-phase
// incident beam
e⁻
Terrace width
10.8 mJ
Pb(111)
573 K - after laser
(b) 9.0 KeV
(00) Beam
<110>
Out-of-phase
// incident beam
Pb(111)
573 K - before laser
Step terrace width (Å)
Laser pulse energy (mJ)
72
62
52
42
32
70
60
50
40
4
6
8
10
12
14
16

Fig. 3

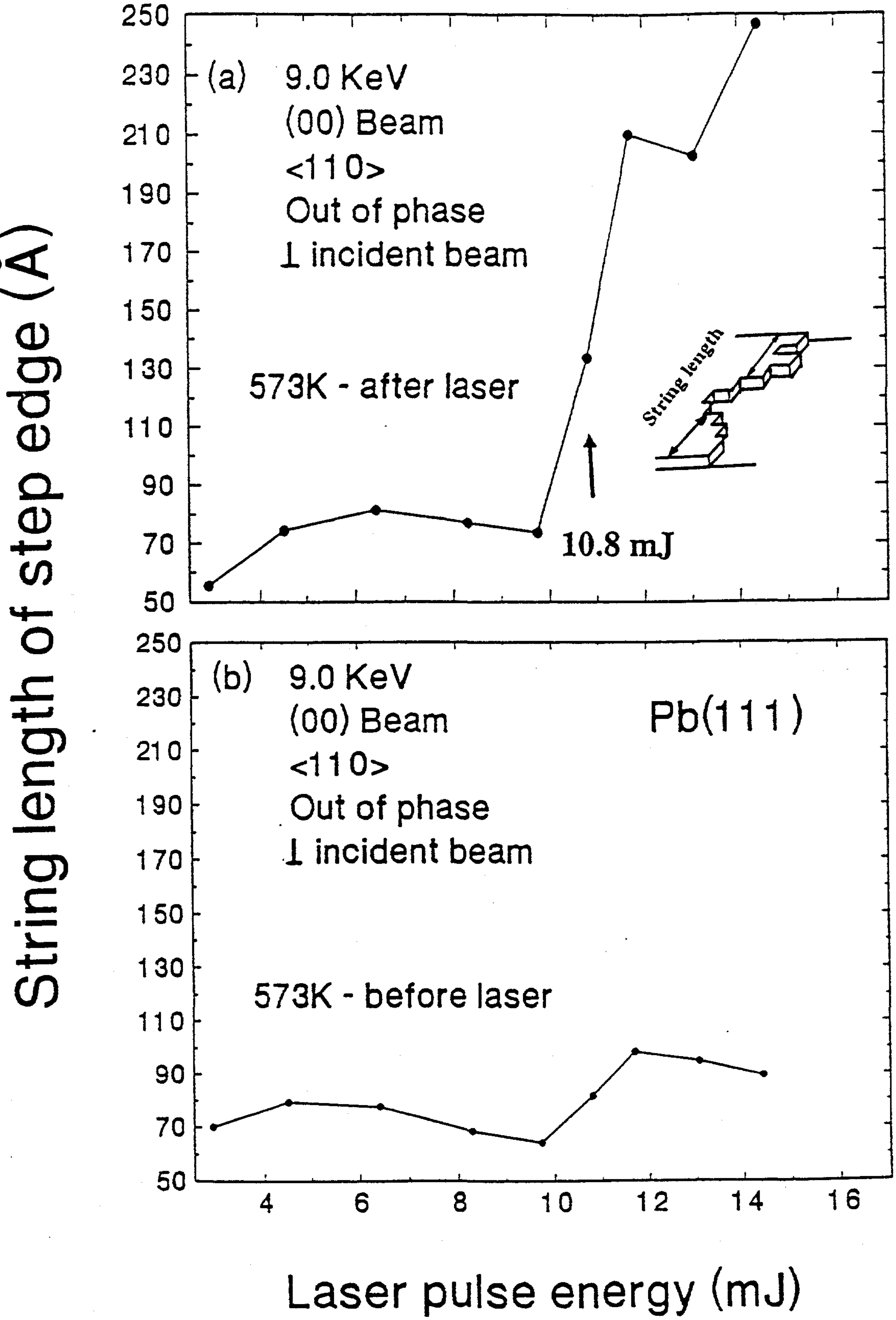

(a)
9.0 KeV
(00) Beam
<110>
Out of phase
⊥ incident beam
573K - after laser
10.8 mJ
String length
(b)
9.0 KeV
(00) Beam
<110>
Out of phase
⊥ incident beam
Pb(111)
573K - before laser
String length of step edge (Å)
Laser pulse energy (mJ)
250
230
210
190
170
150
130
110
90
70
50
4
6
8
10
12
14
16

Fig. 4